

# Evaluation of DAST Crystals for Nonpolarimetric Self-heterodyne Electro-optic Detection of Terahertz Waves

Hai Huy NGUYEN PHAM<sup>†</sup>, Shintaro HISATAKE<sup>†</sup>, Hirohisa UCHIDA<sup>‡</sup>,  
and Tadao NAGATSUMA<sup>†</sup>

<sup>†</sup> Graduate School of Engineering Science, Osaka University 1-3 Machikaneyama, Toyonaka, Osaka, 560-8531 Japan.

<sup>‡</sup> ARKRAY Inc., Yosuien-nai, 59 Gansuin-cho, Kamigyo-ku, Kyoto, 602-0008 Japan.

E-mail: <sup>†</sup> {haihuynguyenpham135}@s.ee.es.osaka-u.ac.jp, <sup>†</sup> {hisatake, nagatsuma}@ee.es.osaka-u.ac.jp

<sup>‡</sup> {uchidah}@arkray.co.jp

**Abstract** The use of a DAST crystal, an organic electro-optic (EO) material with a high EO coefficient, in a nonpolarimetric self-heterodyne EO detection system is studied. The comparison of the signal-to-noise ratio (SNR) and the measurement stability between DAST and ZnTe sensors is presented. The enhancement of the SNR of the amplitude measurement of about 9 dB by the DAST sensor was achieved.

**Keywords** EO sensing, THz, nonpolarimetric, self-heterodyne, DAST sensor

## 1. Introduction

The visualization of electromagnetic (EM) waves in the near-field region has been a strong demand for characterizing and diagnosing devices such as antennas and integrated circuits (ICs) [1, 2]. Especially, in the terahertz (THz; 0.1 – 10 THz) region, the development of a lot of semiconductor devices with metallized interconnections for the practical applications, i.e., ultrafast wireless communication [3, 4] is driving force for the necessity of precise mapping of THz fields around emitters [5]. The electro-optic (EO) detection system has gained a significant research interest for this demand in recent years owing to its large detection bandwidth and negligible field perturbation [6, 7].

Recently, we have developed an EO detection system, which is based on nonpolarimetric and self-heterodyne techniques, to reveal the spatial-temporal evolution of freely propagating continuous THz waves [8]. This system also enabled us to characterize an indoor communication antenna in F-band (90 – 140 GHz) [9].

At higher frequencies of over 300 GHz, the output power of the signal sources decreases. Therefore, it is necessary to enhance the sensitivity or signal-to-noise ratio (SNR) of the system to characterize devices operating at such high frequencies. The use of an EO crystal, which has a larger EO coefficient, such as a 4-dimethylamino-N-methylstilbazolium tosylate (DAST) crystal is one of the promising approaches [10]. However, the birefringence fluctuation induced by the temperature fluctuation in the EO crystal affects the sensitivity of the measurement in a

conventional EO detection system based on polarization modulation technique [11]. In contrast, the nonpolarimetric technique in our system solves an intrinsic problem of the conventional EO detection technique in which the sensitivity of the measurement can be changed by the fluctuation of the polarization state of the probe beam [12]. In this paper, a utilization of a DAST sensor in a nonpolarimetric self-heterodyne system is presented. A comparison of the sensitivity and stability between the DAST and ZnTe sensors is also discussed.

## 2. System configuration

### 2.1 Nonpolarimetric self-heterodyne EO detection system

Figure 1 shows the schematic of our EO detection system. Two free-running 1.55- $\mu\text{m}$  lasers were used for both the generation and detection of THz waves. The frequencies of these lasers were  $f_1$  and  $f_2$  ( $f_2 > f_1$ ). The frequency of laser 1 was shifted by  $f_s$  (100 kHz) by an EO frequency shifter (FS) to realize the self-heterodyne technique. Then two optical sources were coupled by optical coupler and the beat-note was converted to the THz waves ( $f_{\text{THz}} = f_2 - f_1 - f_s$ ) by an optical-to-electrical (O/E) converter, i.e., uni-travelling-carrier photodiode (UTC-PD). In the local oscillator (LO) part, the optical sources were coupled without shifting the frequency. The THz waves (RF signal) emitted from an antenna, a standard F-band horn antenna in our case, modulated the probe beam (LO signal) inside the EO sensor. It only required one sensor for the detection in our system. However, to compare the SNR and stability of the system by ZnTe and DAST sensors, we setup

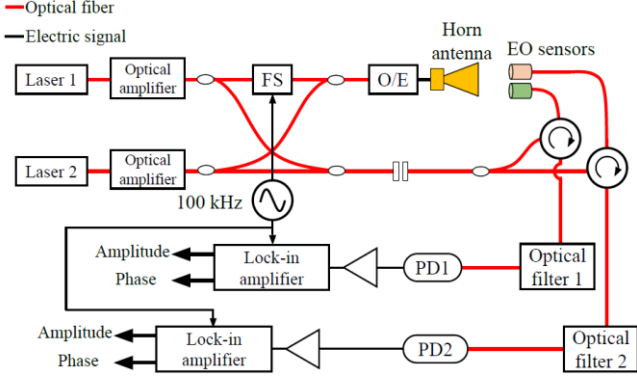


**Fig. 1** Nonpolarimetric self-heterodyne EO detection system. FS: electrooptic frequency shifter, O/E: optical to electrical converter, PD: photodiode.

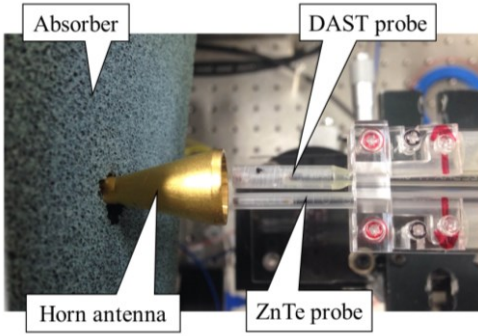


**Fig. 2** The position of sensors in the measurement (top view).

the system with two sensors (Fig.2). Both sensors had the same dimension ( $1 \text{ mm} \times 1 \text{ mm} \times 1 \text{ mm}$ ), mounted on different polarization maintaining fiber (PMF). The probe beam was collimated in the EO crystal by a gradient index (GRIN) lens, and reflected by a high-reflection (HR) mirror to return back to the PMF (Fig.3). The reflected probe beam passed through an optical filter and the signal was detected by photodiode (PD). The amplitude and the phase of the intermediate frequency (IF) signal were measured by lock-in detection.

## 2.2 Principle

Figure 3 shows the principle of our detection technique. The RF frequency is  $f_{\text{THz}} = f_2 - f_1 - f_s$ . In the optical LO signal, there are two frequency components  $f_1$  and  $f_2$ , which are collimated to the EO crystal. These carriers are modulated by an RF signal to generate the sidebands. In Fig.3, the upper sideband of carrier  $f_1$  and the lower sideband of carrier  $f_2$  are presented in the right dash line and the left dash line in the IF box, respectively. Because the frequency of the RF signal is  $f_{\text{THz}} = f_2 - f_1 - f_s$ , the frequency of the sideband of carrier  $f_1$  and carrier  $f_2$  is  $f_2 - f_s$  and  $f_1 + f_s$ , respectively. One pair of the carrier and sideband, in this case, carrier  $f_2$  and sideband

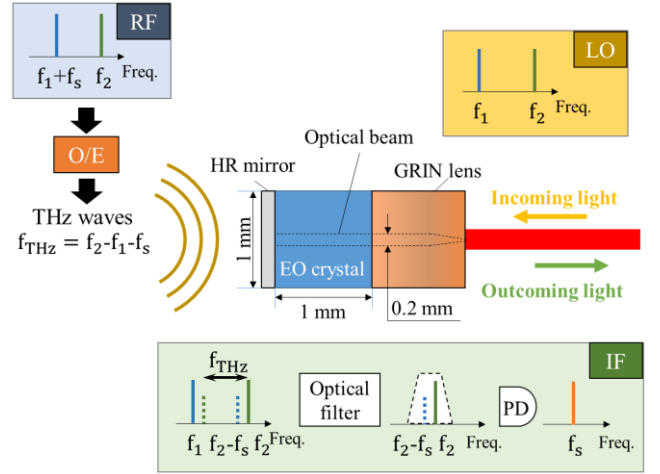


**Fig. 3** Principle of nonpolarimetric self-heterodyne EO detection technique.

**Table 1** Comparison between ZnTe and DAST properties .

	ZnTe	DAST
Optical feature	Isotropic	Biaxial
Refractive index @1550 nm [13]	$n=2.75$	$n_1=2.14$
Relative permittivity (THz region)	$\epsilon_{\text{ZnTe}}=10.1$	$\epsilon_{\text{DAST}}=5.76$
EO coefficient (pm/V) [14]	$r_{41}=4$	$r_{11}=47$ @1535 nm
Sensitivity factor	$SF_{\text{ZnTe}}=8.2$	$SF_{\text{DAST}}=80.0$

$f_2 - f_s$ , is extracted by an optical filter. Then, a PD is used to down-convert the optical sideband  $f_2 - f_s$  to IF signal  $f_s$ . The amplitude and phase of THz waves are simultaneously obtained using lock-in amplifiers.

Table 1 shows the properties of two kind of sensors used in the experiment, ZnTe and DAST sensors. The DAST crystal has a lower permittivity and higher EO coefficient than ZnTe crystal. This leads to the enhancement of the theoretical calculated sensitivity factor of about 9.8 times by the DAST sensor in comparison with the ZnTe sensor as following equations [12]:

$$SF_{\text{DAST}} = r_{11} n_1^3 / \epsilon_{\text{DAST}}, \quad (1)$$

$$SF_{\text{ZnTe}} = r_{41} n^3 / \epsilon_{\text{ZnTe}}, \quad (2)$$

where  $r$ ,  $n$ , and  $\epsilon$  is EO coefficient, refractive index and relative permittivity of the EO crystal as described in table 1, respectively. Note that equation (1) is used for the calculation of the sensitivity for the nonpolarimetric technique. As for the conventional polarimetric technique, the sensitivity factor will be smaller as calculating by following equation [10]:

$$SF_{\text{DAST}} = |r_{11} n_1^3 - r_{21} n_2^3| / \epsilon, \quad (3)$$

where  $n_1$  and  $n_2$  is extraordinary and ordinary refractive index, respectively. Note that the sensitivity factor indicates how big the signal can be detected, it doesn't include the noise in the calculation.

### 3. Experimental results

The difference in frequencies between the two lasers is set at 125 GHz, and measured by an optical spectrum analyzer. The THz power emitted from the horn antenna was about 1.1 dBm and the optical power fed to each sensor was about 13 dBm. The time constant of the lock-in detection was set to 30 ms.

The measured signal at time  $t$  is considered as  $x(t)=S+n(t)$ , where  $S$  and  $n(t)$  are the averaged signal and white noise, respectively. In this condition, the SNR was calculated by following equation [15]:

$$SNR = 20 \log_{10}(\mu/\sigma), \quad (4)$$

where  $\mu=S$  and  $\sigma$  are the mean value and the standard deviation of the detected amplitude signal without moving the sensor. We define the minimum detectable e-field is the value of e-field where the SNR of detected signal is 0 dB corresponding to the mean value equals to the standard deviation ( $\mu=\sigma$ ).

Figure 4(a) and (b) show 1 minute measurement of the amplitude and phase of THz waves detected by the DAST and ZnTe sensors at the same time, respectively. Both amplitude values are normalized to the maximum value of the amplitude obtained by the ZnTe probe. As shown in Fig.4, the measured amplitude by both ZnTe and DAST sensors is stable. However, the measured amplitude by the DAST sensor is about 9 times higher than that obtained by the ZnTe sensor. The SNR of the system using the DAST sensor ( $SNR_{DAST}=47.2$  dB) is about 9 dB higher than that using the ZnTe sensor ( $SNR_{ZnTe}=38.5$  dB), corresponding to the enhancement of the minimum detectable e-field of about 2.8 times from 1.02 V/m to 0.37 V/m. The minimum detectable e-field of a CdTe sensor was reported at 1.0 V/m in reference [6]. This indicates that the DAST sensor offers better minimum detectable e-field than general inorganic sensors when utilizing it in our EO detection system. Table 2 summarizes the mean value, the standard deviation, the SNR of the measured amplitude and the standard deviation of measured phase by both sensors. Even though the detected signal increases 9 times, the noise or standard deviation of the amplitude measurement also increases 2 times ( $\sigma_{aDAST}=79.3$  mV,  $\sigma_{aZnTe}=38.5$  mV). This limits the enhancement of the SNR of the measurement. The phase measurement by the DAST sensor is slightly unstable than that by the ZnTe sensor ( $\sigma_{pDAST}=0.19$  rad,  $\sigma_{pZnTe}=0.17$  rad). The reason for this slight instability of the amplitude and phase measurement by the DAST sensor is needed to be investigated further in the future.

### 4. Conclusion

The utilization of the DAST sensor in the nonpolarimetric self-heterodyne EO detection was

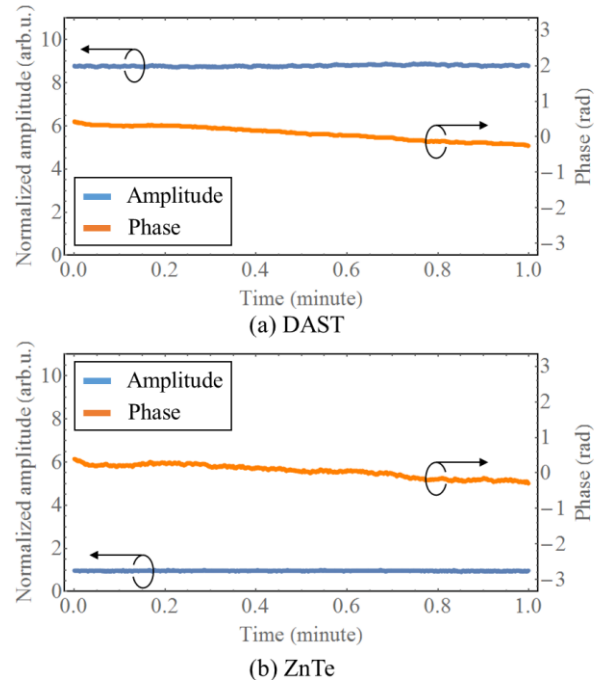


**Fig. 4** (a) and (b) Amplitude and phase of detected signal in 1 minute.

**Table 2** Comparison of detected signal by ZnTe and DAST sensors

	ZnTe	DAST
Averaged amplitude signal (mV)	1988.6	18144.5
Amplitude standard deviation (mV)	23.5	79.3
SNR (dB)	38.5	47.2
Minimum detectable e-field (V/m)	1.02	0.37
Phase standard deviation (rad)	0.17	0.19

proposed for the first time. The detected signal obtained with the DAST sensor is about 9 times better than that obtained with the ZnTe sensor as expected in the theoretical calculation. However, the standard deviation of the measurement by the DAST sensor is slightly larger for both amplitude and phase. It is necessary to investigate further the reason of this slight instability of the DAST sensor. In overall, the SNR of the system is enhanced of about 9 dB by utilizing the DAST sensor. In the future, the visualization and the characterization of an antenna at a high frequency region such as 300 GHz by the DAST sensor will be demonstrated.

### Acknowledgments

This work was supported in part by JSPS KAKENHI (25709028, 15K13383).

### References

- [1] M. Hirose, T. Ishizone, and K. Komiyama, "Antenna pattern measurement using photonic sensor for planar near-field measurement at X band," *IEICE Trans. Commun.*, vol.E87-B, no.3, pp.727-734, March 2004.

- [2] J.J. Lee, E.M. Ferren, D.P. Woolen, and K.M. Lee, "Near-field probe used as a diagnostic tool to locate defective elements in an array antenna," *IEEE Trans. Antennas and Propagation*, vol.36, no.6, pp.884-889, June 1988.
- [3] T. Nagatsuma, S. Horiguchi, Y. Minamikata, Y. Yoshimizu, S. Hisatake, S. Kuwano, N. Yoshimoto, J. Terada, and H. Takahashi, "Terahertz wireless communications based on photonics technologies," *Opt. Express*, vol.21, no.20, pp.23736-23747, September 2013.
- [4] D. Kim, J. Hirokawa, K. Sakurai, M. Ando, T. Takada, T. Nagatsuma, J. Takeuchi, and A. Hirata, "Design and measurement of plate laminated waveguide slot array antenna and its feasibility for wireless link system in the 120 GHz band," *IEICE Trans. Commu.*, vol.E96-B, no.8, pp.2102-2111, August 2013.
- [5] S. Bartalini and P.D. Natale, "Sensors: Mapping terahertz waves," *Nat. Photonics*, vol.9, pp.147-148, February 2015.
- [6] H. Togo, A. Sasaki, A. Hirata, and T. Nagatsuma, "Characterization of millimeter-wave antenna using photonic measurement techniques," *International Journal of RF and Microwave Computer-Aided Engineering*, vol.14, pp.2297, April 2004.
- [7] D.J. Lee and J.F. Whitaker, "An optical-fiber scale electro-optic probe for minimally invasive high-frequency field sensing," *Opt. Express*, vol.16, pp. 21587-21597, December 2008.
- [8] S. Hisatake, H.H. Nguyen Pham, and T. Nagatsuma, "Visualization of the spatial-temporal evolution of continuous electromagnetic waves in the terahertz range based on photonics technology," *Optica*, vol.1, no.6, pp.365-371, November 2014.
- [9] H.H. Nguyen Pham, S. Hisatake, and T. Nagatsuma, "Characterization of an F-band horn antenna based on electro-optic near-field measurements," *IEICE Trans. Electron.*, vol.E98-C, no.8, August 2015.
- [10] H. Togo, H. Uchida, H. Yokota, A. Izumi, T. Nagatsuma, and N. Fukasaku, "Highly sensitive optical electric-field sensor using DAST and its applications," *EuMA Proceedings*, vol.4, pp. 294-301, December 2008.
- [11] A. Garzarella, S.B. Qadri, T.J. Wieting, and D.H. Wu, "The effects of photorefractive on electro-optic field sensors," *J. Appl. Phys.*, vol.97, pp.113108, June 2005.
- [12] S. Hisatake and T. Nagatsuma, "Nonpolarimetric technique for homodyne-type electrooptic field detection," *Appl. Phys. Express*, vol.5, 012701, December 2011.
- [13] B. Cai, T. Hattori, H.H. Deng, K. Komatsu, C. Zawadzki, N. Keil, and T. Kaino, "Refractive index control and grating fabrication of 4-N,N-dimethylamino-N-methyl-4-stilbazolium tosylate crystal," *Jpn. J. Appl. Phys.*, vol.40, pp.L964-L966, September 2001.
- [14] F. Pan, G. Knopfle, C. Bosshard, S. Follonier, R. Spreiter, M.S. Wong, and P. Gunter, "Electro-optic properties of the organic salt 4-N,N-dimethylamino-4'-N'-methyl-stilbazolium tosylate," *Appl. Phys. Lett.*, vol.69, pp.13-15, July 1996.
- [15] M. Naftaly and R. Dudley, "Methodologies for determining the dynamic ranges and signal-to-noise ratios of terahertz time-domain spectrometers," *Opt. Lett.*, vol.34, no.8, pp.1213-1215, April 2009.